Effects of noise on dual Shapiro steps

Bachelor's thesis

presented by

Maximilian Hauke

under the supervision of

Prof. Dr. Fabian Hassler

and

Prof. Dr. Markus Müller

JARA-Institute for Quantum Information

June 30, 2023

Abstract

This thesis studies Bloch osciallations in a Josephson junction operating in the phase-slip regime. We discuss the emergence of dual Shapiro steps of constant current in the current-to-voltage characteristic, when an additional AC voltage is supplied. We obtain analytical and numerical results for the phase-locking on the step. As different kinds of noise occur in a real phase-slip junction, we examine the effects of quasiparticle poisoning and Landau-Zener tunneling on the dual Shapiro steps as two types of noise.

Contents

Abstract **iii**

1 Introduction **1**

2 Phase-slip junction in an ideal setup **3**
2.1 Josephson junction in the phase-slip regime 3
2.2 Phase-slip junction with a real current source 5

3 Emergence of dual Shapiro steps **9**
3.1 Appearance of Bloch oscillations 9
3.2 Phase-locking with an AC drive 11

4 Effects of noise on dual Shapiro steps **19**
4.1 Landau-Zener tunneling 19
4.2 Quasiparticle poisoning 23

5 Conclusion and Outlook **25**

A Proof of stability **27**

Acknowledgements **29**

Bibliography **31**

List of Figures

1.1 Quantum metrology triangle 1

2.1 Realization of a phase-slip junction 3
2.2 Energy spectrum of a phase-slip junction 4
2.3 Circuit diagram of the system with a real current source 5
2.4 Tilted washboard potential 6

3.1 Charge over time 10
3.2 Current flowing through the junction over time 11
3.3 IV curve of the phase-slip junction without an AC drive 12
3.4 IV curve of the phase-slip junction with an additional AC drive . 13
3.5 Visualization of the phase-locking with an AC drive 16
3.6 Dependence of the driving voltage and the step width 17

4.1 Landau-Zener tunneling on dual Shapiro steps 20
4.2 Relaxation at different position on the step 21
4.3 Analytical results of effects of Landau-Zener tunneling 22
4.4 Quasiparticle poisoning on dual Shapiro steps 24
4.5 Relaxation after the poisoning of quasiparticles 24

Chapter 1

Introduction

In 1962 Brian David Josephson predicted the Josephson effect [1], which was experimentally observed in 1963 by Sidney Shapiro via steps of constant voltage, when a microwave tone is applied [2]. The physical dual effect is the Bloch oscillations in small Josephson junctions [3]. Bloch oscillations describe the proportionality of current and frequency via $I = \omega_B e/\pi$ with the Bloch oscillation frequency ω_B. This effect may be a missing element by closing the quantum metrology triangle as further discussed in [4], which is shown in Fig. 1.1.

Bloch oscillations can be observed in a phase-slip junction, which is realized

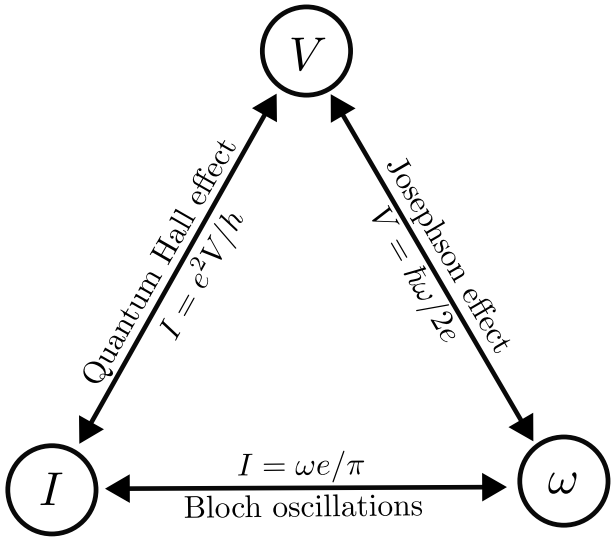

Figure 1.1: Quantum metrology triangle [4]. This triangle allows a self-consistent definition of current, voltage and frequency. The missing link between the current and the frequency may be provided by the Bloch oscillations. Representation according to [5]

by a small Josephson junction, operating in the phase-slip regime. Throughout duality arguments for voltage and current, the emergence of dual Shapiro steps was predicted as the dual counterpart to the known Shapiro steps. Dual Shapiro steps are one way to observe Bloch oscillations by adding an AC drive to the supplied voltage. This leads to steps of constant current, when the Bloch oscillation frequency ω_B reaches an integer multiple of the driving frequency ω_0.

This thesis deals with the characterization of the dual Shapiro steps and we study the effects of noise on these steps. Therefore we introduce the phase-slip junction and its operating regime in Ch. 2. Out of that we obtain a equation of motion, with wich we can describe the Bloch oscillations and the dual Shapiro steps. After that we solve this equation in order to describe Bloch oscillations. Furthermore we gain an analytical understanding of the dual Shapiro steps, without effects of noise (Ch. 3). Finally in Ch. 4 we study the impact of Landau-Zener tunneling and quasiparticle poisoning on the steps, as two different kind of noise.

Chapter 2

Phase-slip junction in an ideal setup

2.1 Josephson junction in the phase-slip regime

This chapter introduces the theoretical background of phase-slip junctions in order to understand dual Shapiro steps. A phase-slip junction can be implemented by a small Josephson junction with a Josephson energy $E_J = \Phi_0 I_c/2\pi$ and a finite capacitance C, where $\Phi_0 = h/2e$ denotes the superconducting flux quantum, with h the Planck constant and e the electron charge. I_c is the critical current, the drive current has to overcome [5]. The realization of the phase-slip junction is shown in Fig. 2.1.

Subsequently it is possible to determine an eigenvalue spectrum by constructing the Hamiltonian of this system and solving it [6]. Figure 2.2 displays the resulting energy spectrum. This spectrum is $2e$-periodic in the charge Q on the

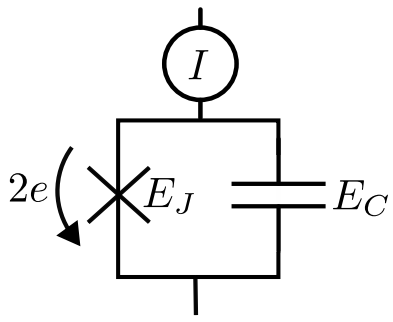

Figure 2.1: Realization of a phase-slip junction with a Josephson junction of energy E_J and a finite capacitance of energy E_C connected to an ideal current source I. Throughout the Josephson junction there is Cooper pair tunneling.

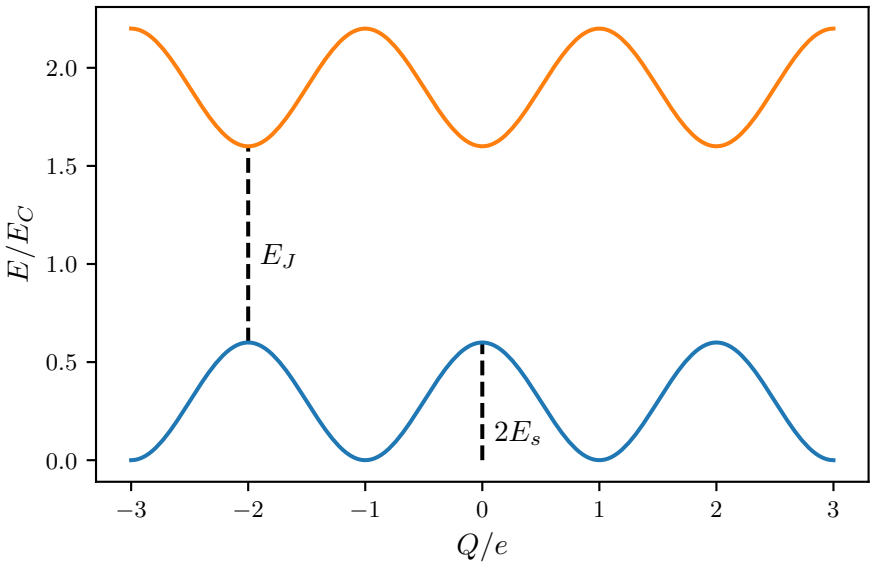

Figure 2.2: Sketch of the energy spectrum of a phase-slip junction for $E_C \lesssim E_J$, which is $2e$ periodic in the charge Q. The band gap scales with the Josephson energy E_J and the energy of the phase-slip junction E_s indicates the height of the lowest band.

capacitor plates. We only consider the regime where $E_C = e^2/2C \lesssim E_J$. For $E_C \ll E_J$ the periodicity of the energy spectrum is negligible and the band structure can be approximated as an harmonic potential. This is the regime, where the Josephson effect can be observed [7]. If $E_C \gg E_J$, the influence of the Josephson junction is negligible, the energy bands will correspond to the bands of nearly free electrons. In the regime, which is more precisely called phase-slip regime, where $E_C \lesssim E_J$, the energy bands are well separated as the energy gap is proportional to E_J [8]. For this reason, we can describe the junction only on the first band of the energy spectrum. In this case, we can approximate the lowest band as an cosine, which yields in

$$E = E_s \cos(\frac{\pi}{e}Q) + E_s. \tag{2.1}$$

The phase-slip energy E_s is the height of the lowest energy band. By deriving the energy spectrum according to the charge, we obtain

$$V = \frac{dE}{dQ} = V_c \sin(\frac{\pi}{e}Q) \tag{2.2}$$

as the equation, which describes the dynamics of the phase-slip junction. The critical voltage $V_c = E_s\pi/e$ is a voltage, which corresponds to the critical cur-

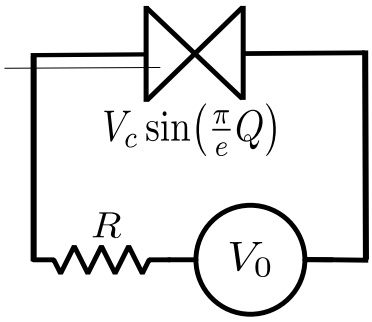

Figure 2.3: Circuit diagram of the system with a real current source, which is implemented by a ideal voltage source, supplying the voltage V_0, and a resistance R. $V_c \sin(\pi Q/e)$ describes the dynamics of the phase-slip junction.

rent I_c of the Josephson junction. Furthermore, a phase-slip junction is the exact dual of the Josephson junction. Therefore, a phase-slip event in a superconducting nanowire changes the phase difference over the wire by 2π, which is the dual process to Cooper-pair tunnelling in a Josephson junction. [9]. The dynamics of the classical Josephson junction model can be described by

$$I = I_c \sin(\phi), \tag{2.3}$$

where the duality of the Josephson junction and the phase-slip junction is evident.

2.2 Phase-slip junction with a real current source

To realize a phase-slip junction in an ideal setup, we take a real current source. This consist of an ideal voltage source and a resistance R, which are connected in series, as shown in Fig 2.3.

Additionally we have to introduce a loop charge operator

$$\hat{Q} = \int_{-\infty}^{t} dt' \hat{I}(t'), \tag{2.4}$$

which indicates the charge going through the junction up to a time t [6]. In order to suppress quantum fluctuations, the resistance R has to be much greater than the quantum resistance $R_Q = h/4e^2$. Therefore the loop charge operator $\hat{Q}$ can be treated as his expectation value Q in a classical way [10].
Subsequently we can derive the equation of motion

$$R\dot{Q} = V_0 - V_c \sin(\frac{\pi}{e}Q) \tag{2.5}$$

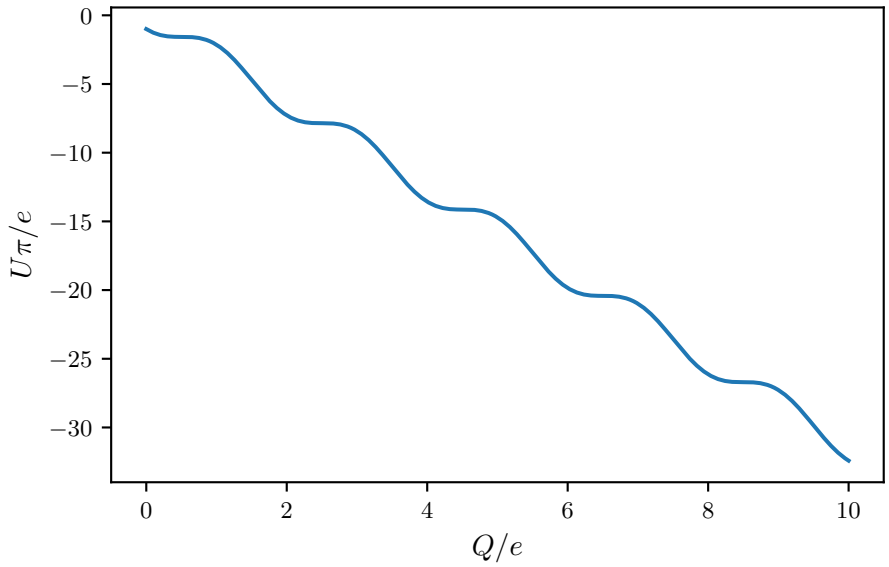

Figure 2.4: Sketch of the tilted washboard potential for $V_0 = V_c$. In this case, the voltage V_0 is exactly high enough to overcome the potential barrier.

of this system via Kirchhoff's law, where V_0 is the voltage supplied by the voltage source. By integrating over the charge Q, we obtain a result for the potential in the phase-slip junction

$$U = -V_0 Q - V_c \frac{e}{\pi} \cos(\frac{\pi}{e} Q). \tag{2.6}$$

This potential is called "tilted washboard potential" which refers to its characteristic shape and is displayed in Fig. 2.4.

From the potential it can also be seen, that there are two different cases, which are interesting to examine later on. Since a voltage V_0 which is below V_c can not overcome the potential barrier, there can not go a current through the phase-slip junction unlike for $V_0 > V_c$.
We now transform Eq. (2.5) into a dimensionless form. For this purpose we introduce $q = \pi Q/e$ as our dimensionless charge. Furthermore we write the voltages in units of V_c, which leads into the notation $v_i = V_i/V_c$. Additionally we define a new timescale by introducing a reference frequency

$$\omega_R = \frac{\pi V_c}{eR} = \frac{1}{RC}, \tag{2.7}$$

which is equal to a RC time in which the motion of the charge is damped. This yields to the non dimensional equation of motion for the charge

$$\frac{\dot{q}}{\omega_R} = v_0 - \sin(q), \tag{2.8}$$

which will be discussed and solved in detail in the following chapter.

Chapter 3

Emergence of dual Shapiro steps

3.1 Appearance of Bloch oscillations

This chapter deals with the analytical and numerical manner of understanding dual Shapiro steps. Dual Shapiro steps occur in the current-to-voltage characteristic (IV curve) of the phase-slip junction while adding an AC drive in oder to observe Bloch oscillations. But before that we turned towards the differential equation in Eq. (2.8)

$$\frac{\dot{q}}{\omega_R} = v_0 - \sin(q),$$

where the voltage source only supplies a DC voltage v_0. Solving this equation results in obtaining the Bloch oscillations.

We now can separately consider the case in which $|v_0| < 1$, so the voltage is below the critical voltage V_c. In this case there are two possible solutions for the differential equation given by

$$q = \arcsin v_0 + 2\pi n, \quad n \in \mathbb{Z}, \tag{3.1}$$

$$q = \pi - \arcsin v_0 + 2\pi n, \quad n \in \mathbb{Z}. \tag{3.2}$$

As we treated in App. A, only the second solution is a stable one. Therefore the charge remains constant over time after an initial response, as shown in Fig. 3.1. Therefore there is no current flowing through the junction in the domain $|v_0| < 1$, because the voltage is too low to overcome the potential

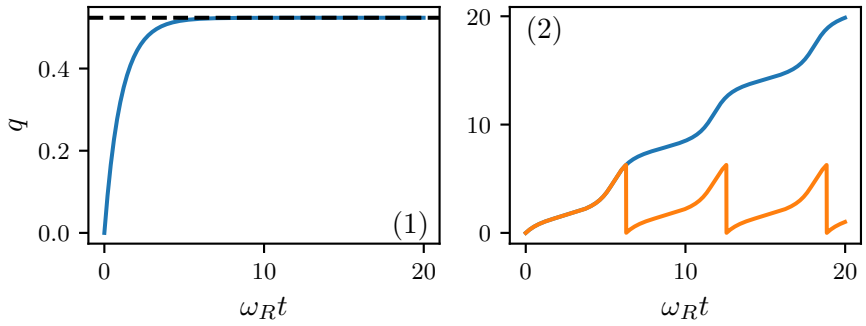

Figure 3.1: Numerical results for the charge over time for different v_0. (1) The figure corresponds to $v_0 = 0.5$, which is below the critical voltage V_c. The curve is approaching a constant value of $\pi + \arcsin v_0$, plotted with the dashed black line. There is no current flowing through the junction. Figure (2) corresponds to the case where $v_0 = \sqrt{2} > 1$. The blue curve shows the numerical result, as the orange one shows the analytical result.

barrier, as shown in Fig. 2.4 by the tilted washboard potential.

Subsequently, we consider the case $|v_0| > 1$. We can solve the equation by separation of variables. Therefore we obtain

$$q(t) = -2 \arctan\left[\frac{1}{v_0}\left(1 - \sqrt{v_0^2 - 1}\tan\left(\frac{\omega_B t + \Theta_0}{2}\right)\right)\right] \tag{3.3}$$

as result for the dimensionless charge. Here, $\omega_B = \omega_R\sqrt{v_0^2 - 1}$ is the Bloch oscillation frequency. In order to fulfill the initial conditions, we introduce a phase Θ_0 of the Bloch oscillations. We again discuss the stability of the solution in App. A. Figure 3.1 displays the numerical as well as the analytical solution. To get a physical result, it is needed to continue the solution analytically over more than one period. In this case the charge, which passed the junction, is getting continuously higher, which does not allow a jump in the analytical solution.

Furthermore it is useful to perform an approximation for a large driving voltage $v_0 \gg 1$. In this domain we get

$$q(t) = \omega_B t + \Theta_0 - \frac{1}{v_0}\cos\left(\frac{\omega_B t + \Theta_0}{2}\right)^2 \tag{3.4}$$

for the dimensionless charge and

$$\dot{q}(t) = \omega_B\left(1 + \frac{1}{2v_0}\sin\left(\omega_B t + \Theta_0\right)\right) + \dot{\Theta}_0 \tag{3.5}$$

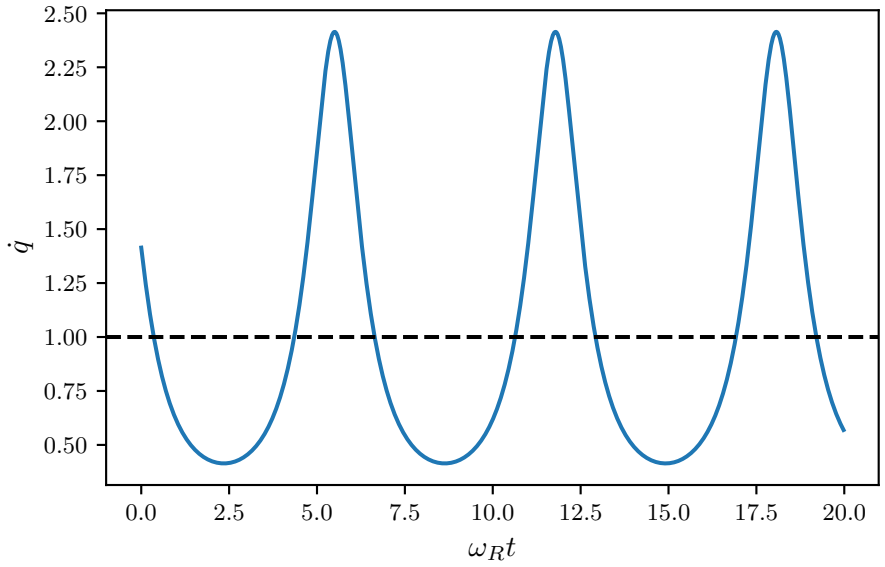

Figure 3.2: Numerical results of the current flowing through the junction over time for $v_0 = \sqrt{2}$. The current is oscillating with the Bloch oscillation frequency which is equal to $\omega_B = \omega_R$ in this special case. The dashed line shows the DC current. This illustrates the current-to-frequency relation $\dot{q}_{DC} = \omega_B/\omega_R$ of the Bloch oscillations.

for the dimensionless current. The current oscillates with the Bloch oscillation frequency ω_B. Figure 3.2 displays the current as well as the corresponding DC current by taking the mean over the time. We obtain the DC current of the Bloch oscillation $I_{DC} = \frac{w_B e}{\pi}$, as shown in figure 3.3.

The numerical results are calculated via the forward Euler method. This is based on discretizing the time into appropriate steps and choosing an initial value $X_0 = X(t = 0)$. After that, the nodal values can be determined via the following algorithm [11]:

$$X_n = X_0 + \sum_{k=1}^{n} f(t_{k-1}, X_{k-1})(t_k - t_{k-1}), \tag{3.6}$$

where $f(X, t)$ is the derivative of X, which we obtain from the differential equation.

3.2 Phase-locking with an AC drive

The previous section dealt with a DC biased phase-slip junction. We now add an AC drive, which corresponds to the influence of microwaves on the junction.

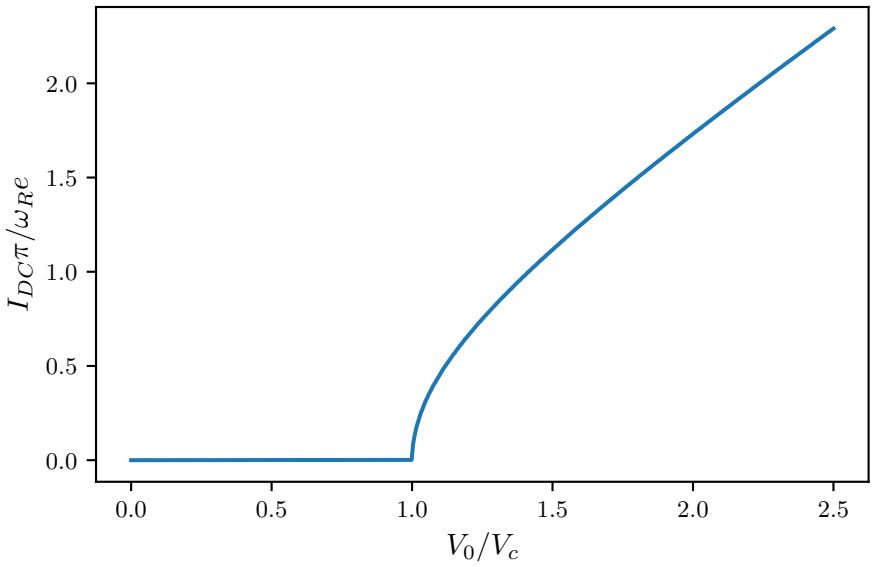

Figure 3.3: IV curve of the phase-slip junction without an AC drive. In the domain below V_C there is no DC current in the junction, as the voltage is too low to overcome the potential barrier. For $v_0 \gg 1$ the current-to-voltage dependence approaches the linear ohmic law.

Therefore the current and the drive can synchronize with each other. This leads to steps of constant current in the IV curve. They occur when the Bloch oscillation frequency ω_B is an integer multiple of the driving frequency ω_0, as shown in figure 3.4.

We characterize these dual Shapiro steps and determine their width in this section. For this purpose we obtain

$$\tilde{V_0} + \Delta V_0 + V_1 \sin(\omega_0 t) = V_c \sin\left(\frac{\pi}{e} Q\right) + R\dot{Q} \tag{3.7}$$

as the new differential equation describing the system, where the voltage source supplies the voltage $V = V_0 + V_1 \sin(\omega_0 t)$. $\Delta V_0 = V_0 - \tilde{V_0}$ indicates the deviation from the voltage

$$\tilde{V_0} = \sqrt{\frac{\omega_0^2}{\omega_R^2} - 1}, \tag{3.8}$$

corresponding to the DC current where $\omega_B = \omega_0$, when the voltage source only supplies a DC voltage. V_1 characterizes the AC drive with driving frequency ω_0. We study the regime of weak driving $V_1 \ll V_c$, because this allows us to

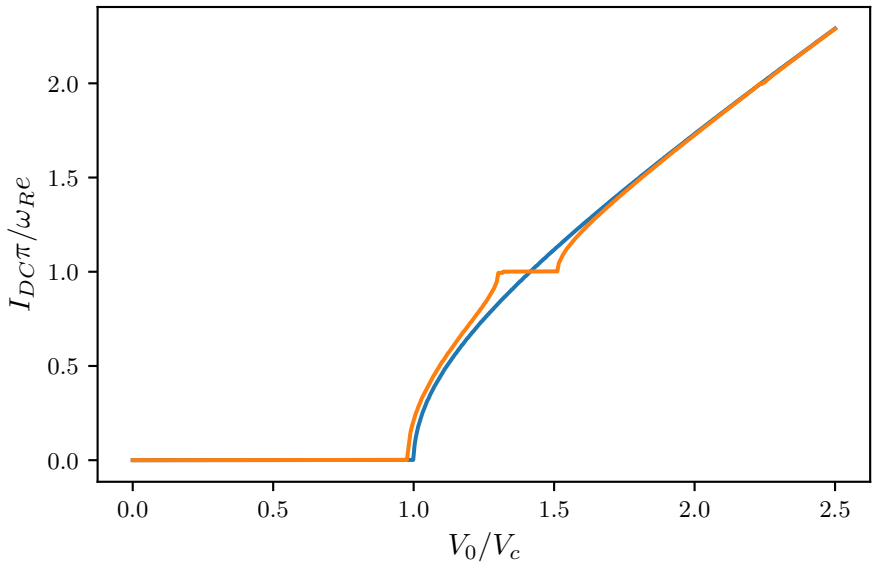

Figure 3.4: IV curve of the phase-slip junction with an additional AC drive of frequency $\omega_0 = \omega_R$ and $V_1 = 0.3V_c$ (orange curve) in comparison to the IV curve without AC drive (blue curve). The dual Shapiro steps occur at multiples of $I_{DC} = \frac{e}{\pi}\omega_0$.

perform a perturbative expansion for the charge $Q = Q_0 + Q_1$, where $Q_1 \ll Q_0$. This yields to two different equations

$$V_0 = V_c \sin\left(\frac{\pi}{e}Q_0\right) + R\dot{Q}_0, \tag{3.9}$$

$$\Delta V_0 + V_1 \sin(\omega_0 t) = V_c \frac{\pi}{e} \cos\left(\frac{\pi}{e}Q_0\right) + R\dot{Q}_1 + R\frac{\dot{\Theta}_0}{\omega_0}\dot{Q}_0, \tag{3.10}$$

from which we solved the first one in the section above, so we can plug in Q_0 from Eq. (3.4) with $\omega_B = \omega_0$, as we want to calculate the behavior on the first step. Furthermore we add a time dependence on the phase Θ_0, as we absorb variation of the frequency into the phase. Due to this we get the last term in the second equation via the chain rule. The time dependence of Θ_0 is very slow in comparison to the driving frequency ω_0. Therefore we can assume $\dot{\Theta}_0$ as constant in the following calculations. $\dot{\Theta}_0$ can be understood as an deviation from the frequency, which leads to a deviation from the current. Furthermore we use the approach, that Q_1 is a linear response with frequency ω_0

$$Q_1 = \mathrm{Re}\left[|\delta Q_1|\, e^{i(\omega_0 t - \Theta_1)}\right]. \tag{3.11}$$

$|\delta Q_1|$ is the amplitude of the response and Θ_1 is the phase shift between the driver and the response.

In order to understand the dual Shapiro steps and to calculate their step width, it is not required to solve the differential equation, but only determine the range in which ΔV_0 is located on the step.
To perform the calculation, it is beneficial to take a mean over the time via the formula

$$\langle f(t)\rangle_{\omega'} = \frac{\omega_0}{2\pi}\int_0^{\frac{2\pi}{\omega_0}} f(t)e^{i\omega' t}dt. \tag{3.12}$$

By evaluating this mean at $\omega' = 0$ and $\omega' = \omega_0$ and performing a high voltage limit $v_0 \gg 1$, we obtain two equations

$$\Delta V_0 = R\frac{e}{\pi}\dot{\Theta}_0 + V_c\frac{\pi}{e}\frac{|\delta Q_1|}{2}\cos(\Theta_0 + \Theta_1), \tag{3.13}$$

$$|\delta Q_1| = -\frac{V_1}{R\omega_0}e^{i\Theta_1}. \tag{3.14}$$

As $|\delta Q_1|$ is a positive and real number, we can now specify
$\Theta_1 = (2n+1)\pi, n \in \mathbb{N}$. Out of this, we get an expression for

$$\Delta V_0 = R\frac{e}{\pi}\dot{\Theta}_0 - \frac{V_c V_1 \pi}{2R\omega_0 e}\cos(\Theta_0). \tag{3.15}$$

On the dual Shapiro step there is a synchronization of the Bloch frequency ω_B with the driving frequency ω_0, which yields in $\omega_B = \omega_0$ on the first step. That means that the additional frequency coming from the phase $\dot{\Theta}_0$ has to vanish.

Via $\dot{\Theta}_0 = 0$, we are able to conclude a relation between the position on the step ΔV_0 and the phase Θ_0. The stability of the solution ist determined by

$$\delta\dot{\Theta}_0 = \sin(\Theta_0)\delta\Theta_0 \tag{3.16}$$

as equation for a small perturbation in the phase on the first step. Out of that we determine the range of the phase Θ_0 on the step to $-\pi \leq \Theta_0 \leq 0$ to reach a stable solution. With this relation, we get an analytical understanding of the phase-locking on the dual Shapiro step. The beginning of the step is connected to $\Theta_0 = -\pi$, where the current and the AC drive are out of phase. This results in the maximal negative power and the junction generates power, which yields in an additive current. For $\Theta_0 = 0$ the drive and the current are in phase, which

is related to the end of the step and results in the maximal positive power. In this case, the junction consumes power and there is a deficit in the current. Figure 3.5 displays the phase relation for three different spots on the step.

With this phase relation, the total step width can be determined to

$$\Delta V = V_1 \frac{\omega_R}{\omega_0}. \tag{3.17}$$

Furthermore, we can see that the step is symmetrical around the center $\tilde{V}_0$.
Subsequently we want to verify our analytical result from Eq. 3.17 with numerical analysis. To determine the step width numerically, we use the method of interval nesting. Therefore we review whether the middle point of a chosen interval lays on the step or not and then bisect the interval. With this method we obtain a result for the left and right end of the step from which we can calculate the step width. Figure 3.6 displays the numerical results for the dependence of ΔV and V_1.
As we can see, there is a non-linear dependence between ΔV and V_1, in contrast to the linear behavior in Eq. (3.17). The deviation from our analytical result is due to our approximation for $V_1 \ll V_c$. For $V_1 \geq V_c$, the AC drive can overcome the potential barrier by itself, which modifies the step width.

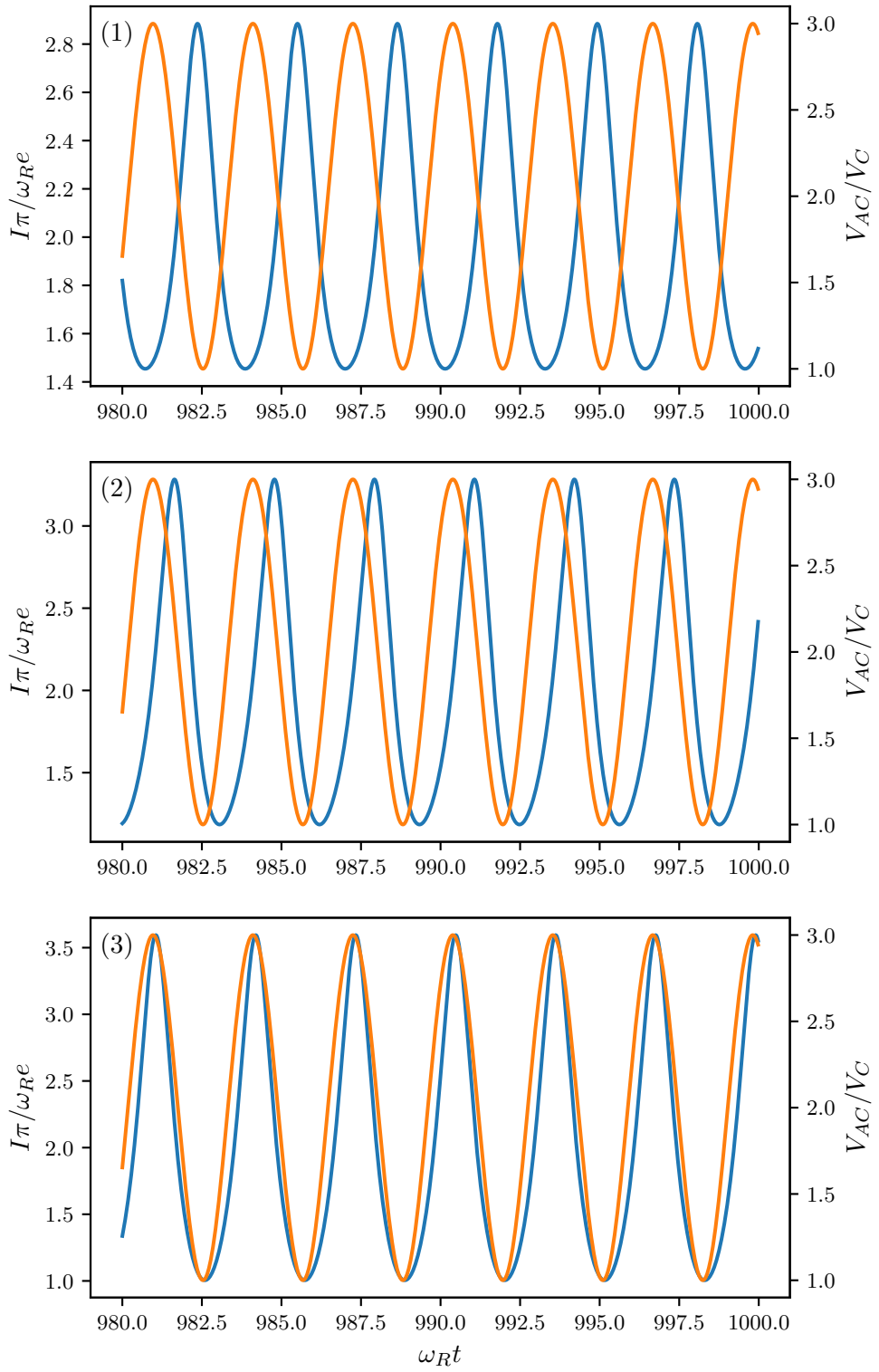

Figure 3.5: Visualization of the phase-locking between the current (blue curve) and the AC drive (orange curve) of frequency $\omega_0 = \omega_R$ and $V_1 = V_c$ after transient response. (1) Current at $\Theta_0 = -\pi$, which corresponds to the left end of the step. At this point the junction generates the maximal power. (2) The middle of the step corresponds to $\Theta_0 = -\frac{\pi}{2}$. (3) At the end of the step the junction consumes the maximal power. At this point the phase is $\Theta_0 = 0$.

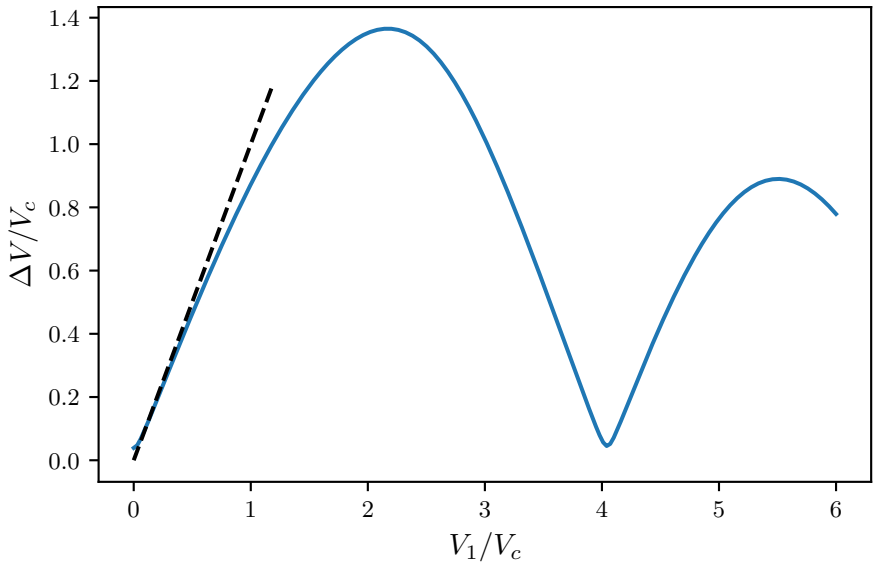

Figure 3.6: Non-linear dependence of the step width ΔV and the driving voltage V_1 in contrast to the linear approximation that derived from our calculations. As we see in the figure, our calculations for the step width are only reasonable for the regime of weak driving $V_1 \ll V_c$.

Chapter 4

Effects of noise on dual Shapiro steps

The previous chapter is based on ideal conditions to observe dual Shapiro steps. Different kinds of noises, which destroy the dual Shapiro steps or change its behavior, were neglected in the previous examinations. In the following chapter, the influences of noise along with its effects on the steps will be analyzed.

4.1 Landau-Zener tunneling

The first type of noise we consider is Landau-Zener tunneling. Landau-Zener tunneling describes the probability of a transition between two separated energy states. This effect and the analytical solution to that was published by Lev Landau [12], Clarence Zener [13], Ettore Mayorana [14] and Ernst Stueckelberg [15] separately at 1932. Therefore it is a non vanishing probability of the system going over to the upper energy level

$$P_{LZ} = \exp\left[-\frac{\pi e \Delta E^2}{4\hbar E_C I}\right] \tag{4.1}$$

for the tunneling event from the first to the second band [16]. ΔE denotes the band gap between the first two energy bands and is approximately equal to E_J.

In order to quantize this phenomena, we use the approach that the second band is from the same form as the lowest energy band, beside of a negative sign. Therefore we obtain

$$E = -E_s \cos(\frac{\pi}{e}Q) + 3E_s + E_J. \tag{4.2}$$

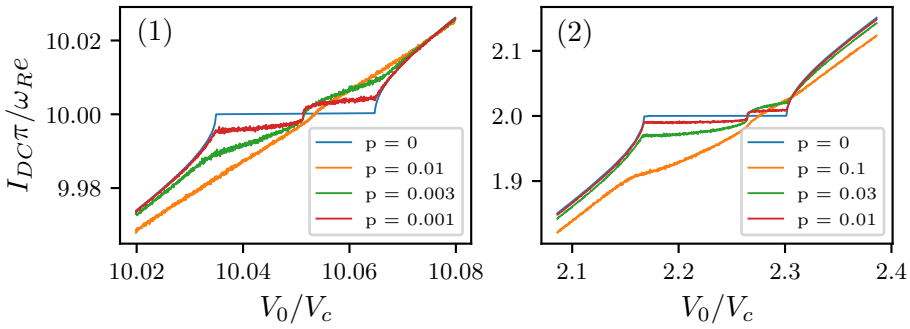

Figure 4.1: Effects of Landau-Zener tunneling on the dual Shapiro step for different probabilities. The AC drive is characterized by $V_1 = 0.3V_c$, and (1) $\omega_0 = 10\omega_R$ as well as (2) $\omega_0 = 2\omega_R$. The Landau-Zener tunneling destroys the steps in dependence of the probability p.

for the second energy band, as we sketched in the Fig. 2.2. The equation of motion on the second band is calculated analogously to Eq. 2.5 to

$$\frac{\dot{q}}{\omega_R} = v_0 + \sin(q). \tag{4.3}$$

This results in a kick of $q' = q + \pi$ for a transition between the two energy bands, as it flips the sign in front of the sine. Since the transition probability is anti proportional to the energy gap, we allow a transition only at the maxima of the lower band, respectively the minima of the higher band. To implement the Landau-Zener tunneling numerically, we allow a transition at $\sin(q) = 0$ and rising edge to the higher band and at $\sin(q) = 0$ and falling edge back to the lower energy band with a chosen probability p.

The effects of Landau-Zener tunneling for different probabilities are displayed in Fig. 4.1.

We can see, that the Landau-Zener tunneling has a huge impact on the steps. The effect of the noise is strongly dependent on the probability p, of which we are poisoning the system. A greater probability leads to a greater deviation from the initial dual Shapiro step. Every event contributes a small additive current, which corresponds to the second half of the step, or a current deficit, which corresponds to the first half of the step. When there is a poisoning event, the system tries to relax into the steady state. Therefore the poisoned system is ahead of the driver and tries to synchronize again in the first half and vice versa. The middle of the step, which is equivalent to $\Theta_0 = \pi/2$, is the voltage, where the behavior flips. After this point, the relaxation is in the

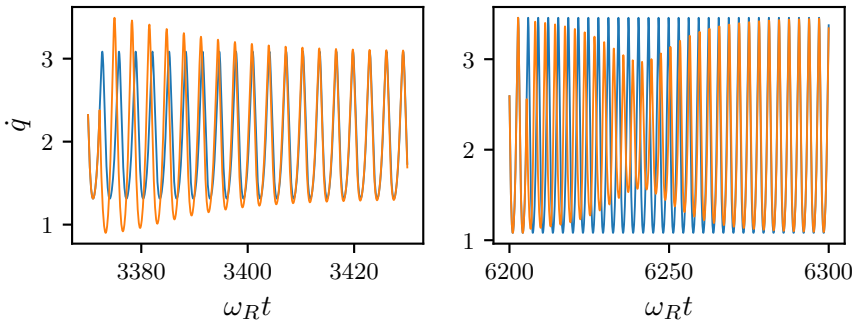

Figure 4.2: Relaxation of the phase at different position on the step. The step, which is characterized by the driving frequency $\omega_0 = 2\omega_R$ and the AC current of $V_1 = 0.3V_c$, is poisoned with a probability of $p = 0.01$. The left figure shows the relaxation for $-\pi \leq \Theta_0 \leq -\pi/2$ and the right one for $-\pi/2 \leq \Theta_0 \leq 0$, where the relaxation goes in the opposite direction. Furthermore the poisoned current is behind the unpoisoned one in the first regime and ahead in the second one.

opposite direction than before this point. Figure 4.2 displays the relaxation at different positions on the step.

Furthermore, there is the goal to gain an analytical understanding of the relaxation. Therefore, we start at Eq. (3.15) and add a kick $\delta\Theta_0$ onto the phase Θ_0. This is since a kick on the charge q is related to a kick on the phase Θ_0 via Eq. (3.3). This results approximately in

$$\delta\dot{\Theta}_0 = \frac{V_1\omega_R^2}{V_c\omega_0}\sin\Theta_0\delta\Theta_0 \tag{4.4}$$

as a differential equation for $\delta\Theta_0$, which we can solve to

$$\delta\Theta_0(t) = \delta\Theta_0(0)\exp\left(\frac{V_1\omega_R^2}{V_c\omega_0}\sin\Theta_0 t\right). \tag{4.5}$$

As we have seen in Fig. 4.2, there is the changing of the additional phase $\delta\dot{\Theta}_0$ that leads to a deviation of the current $I_{DC} \propto \langle\omega_0 + \delta\dot{\Theta}_0\rangle = \omega_0 + \overline{\Delta\omega}$, where we take the mean over $1/\omega_R$.

Therefore we obtain approximately

$$\overline{\Delta\omega} = \delta\Theta_0(0)\omega_R\left(\frac{V_1}{V_c\sqrt{v_0^2 - 1}}\sin\Theta_0\right) \tag{4.6}$$

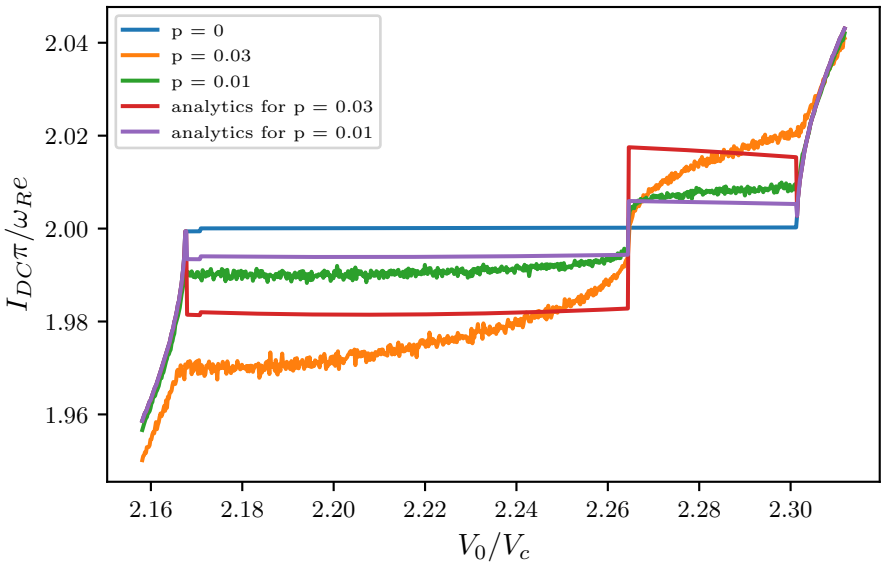

Figure 4.3: Analytical results of the effects of Landau-Zener tunneling for different probabilities and their corresponding numerical results. The AC drive is characterized by $\omega_0 = 2\omega_R$ and $V_1 = 0.3V_c$ and we calculated with the probabilities of $p = 0.03$ and $p = 0.01$.

for $\overline{\Delta\omega}$. We can now plug in our result for Θ_0 on the step from Eq. (3.15), where $\dot{\Theta}_0 = 0$, because of the synchronization on the step. This results in

$$\overline{\Delta\omega} = \delta\Theta_0(0)\omega_R v_1 \sqrt{\frac{1}{v_0^2 - 1} - \frac{\left(v_0 - \sqrt{\frac{\omega_0^2}{\omega_R^2} + 1}\right)^2}{v_1^2}} \tag{4.7}$$

for $\overline{\Delta\omega}$, which is only dependent of parameters, we used in our numerics. For the poisoned current we therefore obtain

$$I_{DC} = I_{DC,0} \pm p\frac{\pi}{e}\overline{\Delta\omega}. \tag{4.8}$$

This result only includes small probabilities as we used the approach, that we only allow one tunneling event within the relaxation time.

Figure 4.3 displays the analytical solution to the effects of Landau-Zener tunneling. As our approach only allows small probabilities, the analytical results differ more from the numerical ones, when going to higher probabilities. To get a better analytical understanding, we had to take account of higher orders, we neglected through our calculation.

In order to minimize the effects of Landau-Zener tunneling we have to maximize the energy band gap to keep the Bloch oscillations on the lowest band.

On the other hand a large Josephson energy $E_J \gg E_C$ results in exiting the phase-slip regime and Bloch oscillations will disappear. Therefore it is needed to find the perfect regime in which Bloch oscillations occur, but the probability of Landau-Zener tunneling is suppressed.

4.2 Quasiparticle poisoning

After considering the effects of Landau-Zener tunneling, we examine the effects of quasiparticle poisoning. Quasiparticles can arise in a phase-slip junction from the absorption of Cooper-pair-breaking photons [17]. Furthermore there is a chance of single-electron tunneling. This effect occur, since there is no perfect superconductor [8]. This kind of noise is probability dependent once again. Therefore there is the Poisson distributed chance of a quasiparticle entering the system with a rate of

$$\Gamma \propto \frac{\Delta E/e^2}{\exp(\Delta E/kT) - 1}, \tag{4.9}$$

where ΔE denotes the difference between the initial and the final state, k the Boltzmann constant and T the temperature [16]. Quasiparticles own a charge of one elementary charge e in contrast to Cooper-pairs with a charge $2e$. Therefore we gain a additional charge, which leads to a shift in the energy spectrum. As our energy spectrum is $2e$-periodic, which we can see in Fig. 2.2, this shift is equivalent to $q = q + \pi$ again. The difference between Landau-Zener tunneling and quasiparticle poisoning is the dependence on the charge, wether a event is allowed or not. This is because quasiparticle poisoning can take place at every time, whereas Landau-Zener tunneling is only allowed at charges, where the energy gap is as low as possible.

We can calculate the effects of quasiparticle poisoning numerically in the same way as we done with the effects of Landau-Zener tunneling. Figure 4.4 displays the numerical results, we obtain for quasiparticle poisoning. The probability p indicates thereby the probability of an event within one period.

Out of that we can see, that the poisoning of quasiparticles has a larger impact on the step than the Landau-Zener tunneling. This is because there is a higher probability of a poisoning event within the relaxation time of a previous one. This leads to longer relaxation times and stronger deflection from the initial curve. Figure 4.5 shows the relaxation after an quasiparticle poisoning event.

The relaxation is very similar to the relaxation after an event of Landau-Zener tunneling. However, the analytical way to understand the effects of quasi-

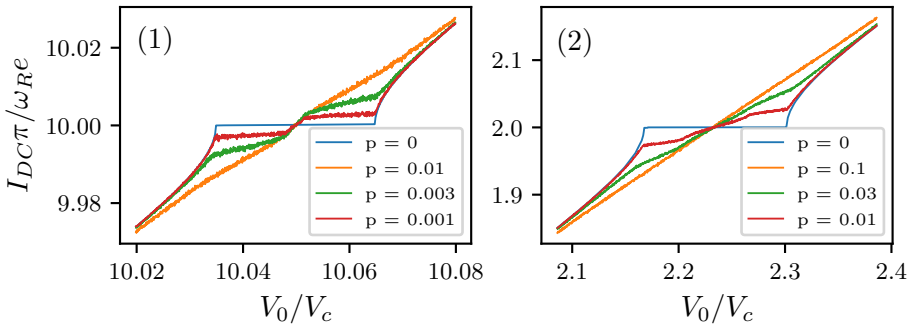

Figure 4.4: Effects of quasiparticle poisoning on the dual Shapiro step for different probabilities. The AC drive is characterized by $V_1 = 0.3V_c$ and $\omega_0 = 10\omega_R$ for the left plot as well as $\omega_0 = 2\omega_R$ for the right one. The quasiparticle poisoning destroys the steps in dependence of the probability p.

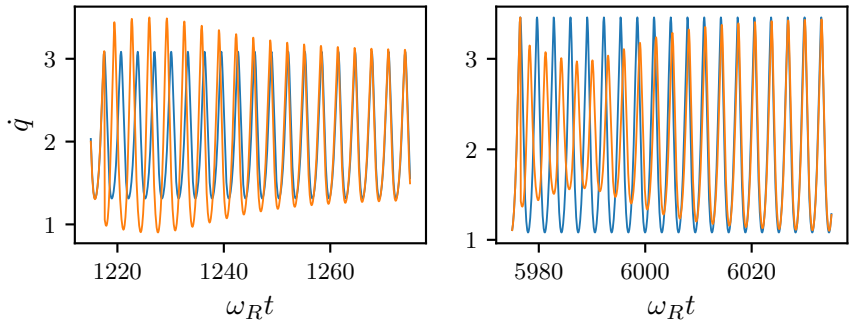

Figure 4.5: Relaxation after the poisoning of quasiparticles with a probability of $p = 0.01$. The AC drive is characterized by $V_1 = 0.3V_c$ and $\omega_0 = 2\omega_R$. The left plot shows the behavior in the regime $-\pi < \Theta_0 < -\pi/2$ and the right one for the regime $-\pi/2 < \Theta_0 < 0$. For the second regime, the relaxation goes into the opposite direction analogously to the effects of Landau-Zener tunneling.

particle poisoning is more difficult. That is due to the charge-to-phase relation, we used in our calculation in the chapter before. As Landau-Zener tunneling takes place at predefined charges, we attain a non-ambiguous related phase, by which the system is shifted. This is different via poisoning with quasiparticles, as events have the probability to take place at any given time.

In order to minimize quasiparticle poisoning, we can lower the temperature, as this would lower the temperature dependent rate in which quasiparticle poisoning occurs. Furthermore, it would reduce the number of quasiparticles due to better superconductivity at lower temperatures.

Chapter 5

Conclusion and Outlook

This thesis has dealt with the effects of different types of noise on dual Shapiro steps. In order to understand dual Shapiro steps, we first introduced the Josephson junction operating in the phase-slip regime in Ch. 2. Out of that we realized a phase-slip junction in an ideal setup and derived the equation of motion of this system.

Furthermore we have studied the appearance of Bloch oscillation in the phase-slip junction with an DC voltage applied in Ch. 3. Under the influence of microwaves, realized via an AC drive, we observed the emergence of dual Shapiro steps. We have gained an analytical understanding of the relation of the phase throughout the step and determined the step width.

In Ch. 4 we studied explicitly the effects of two kind of noises. At first we concerned ourself with the impact of Landau-Zener tunneling. We have gained an understanding of these effects due to our numerical results. Furthermore we determined a solution for the deviation of the current by mentioning the relaxation of the phase. After that, we have determined the influences of quasiparticle poisoning. We obtained a numerical way to understand the effects, but our analytical correction from the calculation of Landau-Zener tunneling did not fit the poisoning with quasiparticles well, as the system is less predictable.

As our analytical results for the effects of noise did not match very well with our numerical results due to higher orders, which we neglected throughout our calculation, this may be an interesting subject for future research. Especially higher orders of the probability may lead to a better characterization of the impact of noise. Futhermore the effect of quasiparticle poisoning is analytically

still undetermined. Therefore it may be interesting to research the relation between the charge and the phase more in detail in the future.

Appendix A

Proof of stability

In this appendix we proof the stability of our solutions for the charge q, while the voltage source is only supplying a DC-voltage of v_0. In order to proof the stability we add a small deflection δq onto our original solution. Therefore we get

$$\dot{q} + \delta\dot{q} = f(q + \delta q) = f(q) + \delta q f'(q), \tag{A.1}$$

with $f(q) = \omega_r(v_0 + \sin(q))$, as equation for δq via a Taylor expansion around $\delta q = 0$. Out of that we obtain two differential equation for $v_0 < 1$ by plugging in our solutions for q out of Eq. (3.1) and Eq. (3.2)

$$\delta\dot{q} = \omega_R \cos(-\arcsin v_0)\ \delta q = \omega_R\sqrt{v_0^2 - 1}\ \delta q, \tag{A.2}$$

$$\delta\dot{q} = \omega_R \cos(\pi + \arcsin v_0)\ \delta q = -\omega_R\sqrt{v_0^2 - 1}\ \delta q. \tag{A.3}$$

Since only in the second equation the factor in front of δq is negative on the whole domain, this is the stable solution of the two.
Analogously we proof the stability of the solution for $v_0 > 1$. This results in

$$\delta\dot{q} = \frac{1}{\omega_R}\cos\left[2\arctan\left(\frac{1}{v_0}\left(1 - \sqrt{v_0^2 - 1}\tan\left(\frac{\omega_B t + \Theta_0}{2}\right)\right)\right)\right]\delta q \tag{A.4}$$

as differential equation for δq. In this case $f'(q)$ seems to be periodical around zero, which implies that there is neither a relaxation to a stable solution nor an unstable solution. In order to verify that, we calculate the integral over one period $T = 2\pi/\omega_B$. For that, we calculate a root of $f'(q)$

$$t_0 = \frac{1}{\omega_B}\left[2\arctan\left(\frac{v_0 + 1}{\sqrt{v_0^2 - 1}}\right) - \Theta_0\right] \tag{A.5}$$

and shift the whole function by t_0, because the shifted function is odd at $t = 0$. Subsequently we can take advantage of the periodicity of $f'(q)$ and move the limits of the integral by $T/2$, which leads to symmetrical limits. Therefore we get zero for the integral we have to determine. This proves, that δq stays a constant deflection.

Acknowledgements

I would like to express my sincere gratitude to all those who have contributed to the successful completion of this Bachelor's thesis. Without their invaluable support, guidance, and encouragement, this accomplishment would not have been possible.

First i would like to thank Fabian Hassler for introducing me into this interesting branch of physics. His expertise, insightful feedback, and constant encouragement throughout this research journey has been instrumental in shaping the direction of this thesis.

No less I would like to thank David Scheer for always being available for questions and discussions. I could always rely on his advice and experience. Many thanks for all the time he dedicated to me and my work in order to support me.

Last but not least, I would like to thank my family, friends, and girlfriend Sophia for their support and constant encouragement throughout my academic journey.

In conclusion, I would like to thank everyone who has played a role, big or small, in the successful completion of this Bachelor's thesis. Their support, guidance, and encouragement have been invaluable, and I am truly grateful for the contributions.

Bibliography

[1] Josephson, B. *Possible new effects in superconductive tunnelling.* In Phys. Lett., 1(7), 251–253, 1962.

[2] Shapiro, S. *Josephson currents in superconducting tunneling: The effect of microwaves and other observations.* In Phys. Rev. Lett., 11(2), 80–82, 1963.

[3] Averin, D., Zorin, A. and Likharev, K. *Bloch oscillations in small josephson junctions.* In Sov. Phys. JETP, 61(2), 407–413, 1985.

[4] Pekola, J. P., Saira, O.-P., Maisi, V. F., Kemppinen, A., Möttönen, M., Pashkin, Y. A. and Averin, D. V. *Single-electron current sources: Toward a refined definition of the ampere.* In Rev. Mod. Phys., 85, 1421–1472, 2013.

[5] Arndt, L. *Dual Shapiro steps of a phase-slip junction in the presence of a parasitic capacitance.* Master's thesis, RWTH Aachen University, 2018.

[6] Ulrich, J. and Hassler, F. *Dual approach to circuit quantization using loop charges.* In Phys. Rev. B, 94(9), 2016.

[7] Crescini, N., Cailleaux, S., Guichard, W., Naud, C., Buisson, O., W. Murch, K. and Roch, N. *Evidence of dual Shapiro steps in a Josephson junction array.* In Nature Physics, 19(6), 851–856, 2023.

[8] Geigenmüller, U. and Schön, G. *Single electron effects and Bloch oscillations in normal and superconducting tunnel junctions.* In Physica B: Condensed Matter, 152(1), 186–202, 1988.

[9] Mooij, J. E. and Nazarov, Y. V. *Superconducting nanowires as quantum phase-slip junctions.* In Nature Physics, 2(3), 169–172, 2006.

[10] Masluk, N. A., Pop, I. M., Kamal, A., Minev, Z. K. and Devoret, M. H. *Microwave characterization of Josephson junction arrays: Implementing a low loss superinductance.* In Phys. Rev. Lett., 109, 137002, 2012.

[11] Estep, D. *The Forward Euler Method*, pp. 583–604. Springer New York, New York, NY, 2002.

[12] Landau, L. D. *Zur Theorie der Energieübertragung. ii.* In Physics of the Soviet Union, 1932.

[13] Zener, C. *Non-adiabatic crossing of energy levels.* In Proc. R. Soc. Lond. A, 137, 696–702, 1932.

[14] Majorana, E. *Atomi orientati in campo magnetico variabile.* In Il Nuovo Cimento (1924-1942), 9(2), 43–50, 1932.

[15] Stueckelberg, E. *Theorie der unelastischen Stösse zwischen Atomen.* In Helvetica Physica Acta, 1932.

[16] Vora, H., Kautz, R. L., Nam, S. W. and Aumentado, J. *Modeling Bloch oscillations in nanoscale Josephson junctions.* In Phys. Rev. B, 96, 054505, 2017.

[17] Liu, C.-H., Harrison, D. C., Patel, S., Wilen, C. D., Rafferty, O., Shearrow, A., Ballard, A., Iaia, V., Ku, J., Plourde, B. L. T. and McDermott, R. *Quasiparticle poisoning of superconducting qubits from resonant absorption of pair-breaking photons.* In arXiv:2203.06577, 2022.